Theoretical and Applied Climatology (2026) 157:28
https://doi.org/10.1007/s00704-025-05972-4

RESEARCH

Thermal persistence index (TPI): a novel measure of prolonged heat stress in the Mediterranean, 1950–2024

Doğukan Doğu Yavaşlı[1]

Received: 30 September 2025 / Accepted: 9 December 2025 / Published online: 20 December 2025

Abstract
The Mediterranean basin is a prominent 'hotspot' highly vulnerable to anthropogenic climate change, where heatwaves are increasing in frequency, intensity, and duration. Traditional heat stress metrics, often focusing on instantaneous conditions or daily averages, fail to capture the cumulative impact of uninterrupted intra-daily exposure. In this study, we introduce the Thermal Persistence Index (TPI), a novel metric quantifying the persistence of human-relevant heat stress on an hourly scale. TPI is defined as the maximum number of consecutive hours within a day during which the Universal Thermal Climate Index (UTCI) exceeds + 32 °C ('strong heat stress'). Using ERA5-Land reanalysis (1950–2024), we analyze long-term trends, regime shifts, and spatial hotspots for three TPI-derived metrics: seasonal mean (tpi_mean), seasonal maximum (tpi_max), and days with TPI ≥ 6 h (tpi_ge6days). Results reveal widespread, statistically significant increases in all metrics, with consensus hotspots in eastern Spain, northern Italy, the Aegean, and the Levant. Pettitt change-point analysis identifies the 1990s—particularly 1997—as the dominant period of regime shift. These findings indicate that the Mediterranean has entered a new thermal regime characterized not only by hotter days but also by longer and more frequent periods of intra-daily heat stress. TPI offers a concise framework for assessing climate-driven changes in heat stress duration and supporting targeted adaptation in public health, labor, and agriculture.

Keywords Mediterranean climate change · Universal Thermal Climate Index (UTCI) · Heat stress persistence · Extreme temperature trends

1 Introduction

Anthropogenic climate change has caused a significant increase in the frequency, severity, and duration of hot extremes globally, with the Mediterranean basin emerging as a particularly vulnerable hotspot where these trends have accelerated over recent decades (Pastor et al. 2024; Perkins et al. 2012). Numerous studies indicate that heatwaves and warm spells have become significantly more frequent and longer-lasting since the mid-20th century, driven by amplified regional warming that often exceeds the global mean and produces prolonged heat episodes surpassing 40 °C in southern and eastern Mediterranean sectors (Perkins-Kirkpatrick and Lewis 2020; Wang et al. 2024; Luo et al. 2024; Marx et al. 2021). Marine heatwaves intensify regional warming by raising sea-surface temperatures, which amplifies atmospheric extremes and ecological disruptions, including wildfires. Increased evaporation elevates humidity, reducing the body's capacity for evaporative cooling and thereby prolonging heat stress exposure (Guiot and Cramer 2021). Projections under high-emission scenarios indicate that heatwave durations will lengthen further, with urban areas experiencing exacerbated stress due to the urban heat island effect, thereby heightening risks to human health, agriculture, and infrastructure (Founda and Giannakopoulos 2024). The consequences of prolonged extreme heat are already evident: the extraordinary European heatwave of 2003 persisted for weeks and resulted in over 70,000 excess deaths (García-Herrera et al. 2010), while the Russian heatwave of 2010 lasted nearly two months and caused tens of thousands of fatalities alongside widespread wildfires (Di Capua et al. 2021). Beyond acute mortality, sustained high temperatures impair economic productivity: during the 2013–2014 Australian summer, heat stress caused labor losses estimated at

✉ Doğukan Doğu Yavaşlı
dogukan.yavasli@ahievran.edu.tr

[1] Department of Geography, Kırşehir Ahi Evran University, Kırşehir, Turkey

US$6.2 billion, equivalent to 0.33–0.47% of GDP (Zander et al. 2015).

The physiological burden of sustained heat exposure extends beyond immediate discomfort. When ambient conditions exceed the body's capacity for heat dissipation, core temperature rises, triggering cardiovascular strain as the heart works harder to increase peripheral blood flow for cooling (Kjellstrom et al. 2009). Prolonged exposure impairs cognitive function, reduces manual dexterity, and increases accident risk, with productivity declining by approximately 2% per degree above optimal conditions (Dunne et al. 2013). Outdoor workers in agriculture, construction, and tourism are particularly vulnerable, as their occupational demands preclude avoidance behaviors available to indoor workers (Flouris et al. 2018). The economic toll is substantial: the International Labour Organization estimates that heat stress will cause the equivalent of 80 million full-time job losses globally by 2030, with Mediterranean and tropical regions bearing the greatest burden (ILO 2019). These impacts underscore the need for metrics that quantify not only the intensity of heat stress but also its temporal persistence, as recovery failure compounds physiological strain and economic losses. A distinctive aspect of this regional warming is the diurnal asymmetry, with nighttime minimum temperatures rising faster than daytime maximum temperatures. This narrowing of the diurnal temperature range (DTR) has been documented across the Mediterranean and globally, limiting nocturnal cooling and thereby reducing the physiological recovery needed after hot days (Jay et al. 2021; Seltenrich 2023; Li et al. 2023; Zhong et al. 2025a, b). Mediterranean observations confirm increasing frequencies of tropical nights (minimum temperature > 20 °C), particularly between June and September, which compound thermal stress and correlate with elevated mortality from cardiovascular and respiratory conditions (Yavaşlı and Erlat 2024; Pradhan et al. 2022; Katavoutas et al. 2022).

To assess heat stress risks, meteorologists and public health agencies traditionally rely on indices such as the Heat Index and Humidex, which combine air temperature and humidity to reflect apparent ("feels-like") temperature, and the Wet-Bulb Globe Temperature (WBGT), widely applied in occupational health as it incorporates temperature, humidity, wind, and radiation (Clark and Konrad 2024). While effective for operational warnings, these indices describe instantaneous conditions and fail to capture the cumulative stress of multi-day exposure. Epidemiological evidence shows that sequences of moderately hot days may produce disproportionately severe impacts on morbidity and mortality when recovery time is insufficient, especially if nights remain warm (Lee et al. 2015; Jay et al. 2021; Seltenrich 2023).

Recognizing the importance of duration, climate research has incorporated time-based criteria into definitions of extremes. The World Meteorological Organization defines a heatwave as at least two consecutive days of abnormally hot weather (Nairn and Fawcett 2011). The ETCCDI indices include TX90p and TN90p (days exceeding the 90th percentile of maximum and minimum temperatures, respectively), as well as the Warm Spell Duration Index (WSDI), which counts days within spells of ≥6 consecutive warm days (Zhang et al. 2005). Mediterranean studies using these indices consistently report increasing warm days, nights, and spells, alongside declining cold extremes (Dong et al. 2023; Katavoutas et al. 2022; Yavaşlı and Erlat 2024). However, these daily metrics do not fully resolve how sustained heat-humidity combinations accumulate within the day and across day-night cycles, limiting their ability to capture sub-daily persistence.

To overcome such gaps, new composite indices have been proposed. In Australia, the Excess Heat Factor (EHF) combines short and long-term moving averages to reflect both intensity and anomaly and has proven to better predict health outcomes than simpler measures (Nairn and Fawcett 2015; Scalley et al. 2015). Similarly, the Accumulated Heat Stress Index (AHI) accounts for thermal load over 72 h, effectively penalizing consecutive hot days and identifying dangerous conditions overlooked by one-day metrics (Lee et al. 2015). These advances underscore that thermal persistence requires dedicated quantification. Table 1 summarizes the key characteristics of widely used heat stress indices, highlighting their temporal resolution, input variables, and primary applications. Notably, none of the existing indices explicitly quantify the duration of consecutive hourly exceedances within a day, a gap that the present study

Table 1 Comparison of heat stress indices by Temporal resolution, input variables, and application domain

Index	Time Scale	Variables	Threshold	Application
WBGT	Instantaneous	T, RH, Wind, Radiation	28 °C	Occupational health
Heat Index	Instantaneous	T, RH	Variable	Public weather warnings
UTCI	Hourly	Full energy budget	32 °C	Thermal comfort
WSDI	Daily	Tmax	90th pctl	Climate monitoring
EHF	3-day	T anomaly	Anomaly	Heatwave detection
AHI	72-hour	T accumulation	Variable	Cumulative stress
TPI	**Intra-daily**	**UTCI-based**	**32 °C**	**Hourly persistence**

addresses. Recent global datasets like GloUTCI-M (Yang et al. 2024) also highlight increasing UTCI trends, supporting the need for persistence-focused metrics in hotspots like the Mediterranean.

In this study, we introduce the Thermal Persistence Index (TPI), a novel metric designed to quantify the persistence of human-relevant heat stress. TPI is defined as the maximum number of consecutive hours within a day during which UTCI exceeds + 32 °C, ranging from 0 to 24 h/day. This formulation directly links to bioclimatic stress thresholds and captures how long heat stress endures within each day. By isolating persistence, TPI complements existing intensity-focused indices such as UTCI, Humidex, or WBGT and provides a standardized basis for evaluating prolonged exposure across diverse climates. Using the ERA5-Land reanalysis, which offers hourly, high-resolution (~9 km) surface variables since 1950 (Muñoz-Sabater et al. 2021), we compute TPI across the Mediterranean basin for May-September, 1950–2024, and analyze its long-term trends. This represents the first systematic application of an hourly persistence index at the basin scale, advancing methods to assess heat risks in a rapidly warming region.

2 Data and methods

We focus on the Mediterranean basin, adopting the IPCC AR6 "MED" reference region as the geographical template. For computational simplicity and reproducibility, this domain was approximated by a rectangular window spanning 30–45° N and −10–40° E, which encompasses the principal land areas used in AR6 regional syntheses and the Interactive Atlas (Iturbide et al. 2020). As the primary dataset, we used the ERA5-Land reanalysis at hourly ~ 0.1° (~ 9 km) resolution for the warm season months of May-September during the period 1950–2024 (Muñoz-Sabater et al. 2021). ERA5-Land provides near-surface meteorological fields consistently forced by ERA5 and elevation-corrected for land applications. From the monthly NetCDF files (YYYY-MM.nc), we extracted the following variables: 2-m air temperature (t2m), 2-m dewpoint temperature (d2m), 10-m winds (u10, v10), downward shortwave and longwave radiation at the surface (ssrd, strd), and surface pressure (sp).

Hourly UTCI values were computed at each grid cell using the operational UTCI polynomial as implemented in pythermalcomfort, which is based on the Fiala multi-node thermoregulation model and adaptive clothing assumptions (Bröde et al. 2012; Fiala et al. 2012; Tartarini and Schiavon 2020). Air temperature was taken from t2m (converted from Kelvin to Celsius), while relative humidity was derived from t2m and d2m using a Magnus/Tetens formulation (Bolton 1980). Wind speed was calculated as the vector magnitude of u10 and v10, consistent with the UTCI reference height. Mean radiant temperature (Tmrt) was estimated from the shortwave and longwave fluxes using a radiation-to-Tmrt conversion constrained by solar geometry and surface radiative balance. To illustrate the behavior of UTCI relative to air temperature, we provide a schematic diurnal comparison for summer and winter conditions (Fig. 1). This example highlights the added influence of radiation, humidity, and wind: in summer, UTCI rises more steeply and exceeds air temperature during midday, crossing the 32 °C threshold for several hours, whereas in winter it remains lower due to

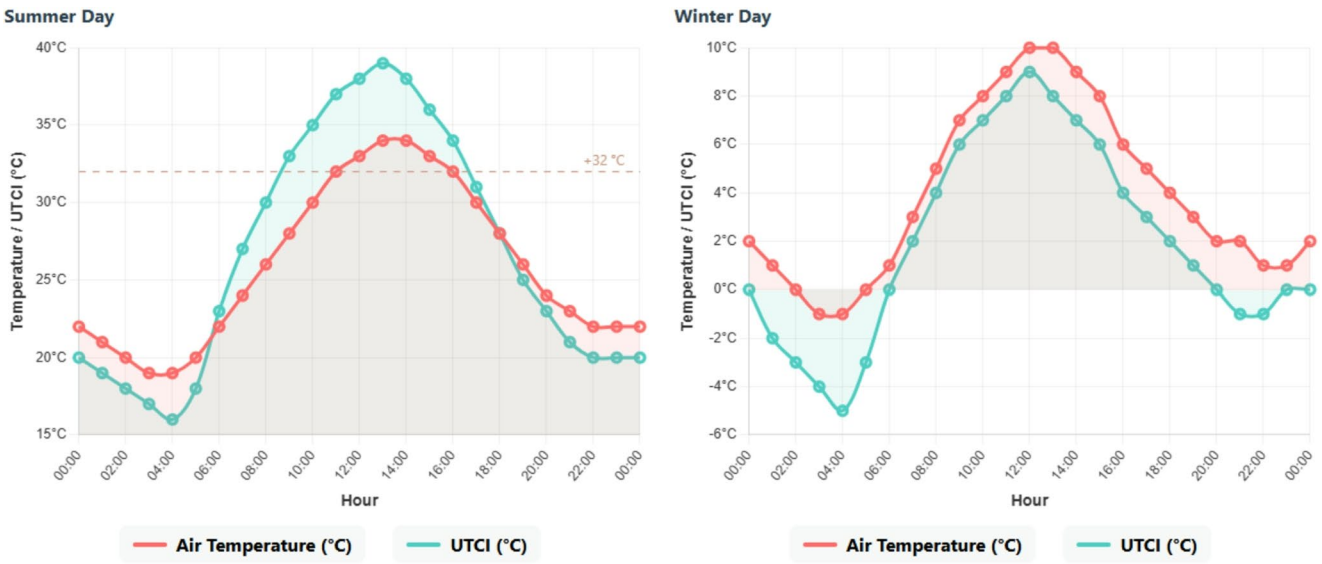

Fig. 1 Idealized diurnal cycles of air temperature and UTCI for summer (left) and winter (right). UTCI diverges from air temperature during midday in summer due to solar radiation and low wind, while in winter it remains lower, reflecting wind chill and reduced radiative forcing

wind chill and reduced radiative forcing. These differences emphasize that UTCI captures multiple drivers of human thermal stress beyond temperature alone. To ensure physical consistency across the domain, plausibility bounds were applied to avoid unrealistic extremes, and quality checks confirmed that UTCI ranges aligned with published values for the Mediterranean region (Bröde et al. 2012; Di Napoli et al. 2019).

To quantify persistence, we defined the Thermal Persistence Index (TPI) as the maximum number of consecutive hours within a calendar day (00:00–23:00 local time) during which UTCI exceeds + 32 °C. This threshold corresponds to the onset of 'strong heat stress' in the standard UTCI classification, above which cardiovascular strain, impaired thermoregulation, and elevated mortality risk have been consistently documented (Bröde et al. 2012; Di Napoli et al. 2021; Blazejczyk, et al. 2012). By design, TPI ranges from 0 to 24 h day^{-1}, where TPI = 0 indicates no hour exceeded the threshold and TPI = 24 indicates continuous exceedance throughout the day. The index captures the longest uninterrupted duration of physiologically relevant heat stress within each day, complementing intensity-focused metrics by explicitly quantifying temporal persistence. This threshold has been widely adopted in health-impact applications, where risks to human health increase substantially above this level (Di Napoli et al. 2021; Charalampopoulos et al. 2024). Because UTCI ≥ 32 °C in the Mediterranean occurs almost exclusively in late spring, summer, and early autumn, the analysis was restricted to May-September to capture the core heat-stress season and to avoid spurious persistence outside it. For each grid cell and day, the longest uninterrupted sequence of hours above the threshold was identified and recorded as the daily TPI (0–24 h day^{-1}). These daily values were further aggregated into three seasonal indices per year: (i) the seasonal mean of daily TPI (tpi_mean; units: h day^{-1}), (ii) the seasonal maximum of daily TPI (tpi_max; h day^{-1}), and (iii) the seasonal number of days with TPI ≥ 6 h (tpi_ge6days; days season^{-1}). Together, these indices characterize the central tendency, extremes, and frequency of prolonged sub-daily heat stress.

For each grid cell and each metric, annual time series spanning 1950–2024 were constructed. Long-term tendencies were estimated using the Theil-Sen median slope, a robust trend estimator insensitive to outliers (Sen 1968). Statistical significance of monotonic trends was tested with the non-parametric Mann-Kendall test at $\alpha = 0.05$ (Mann 1945; Kendall 1948). To detect potential regime shifts, we further applied the Pettitt change-point test (Pettitt 1979) and recorded the most likely year of change when significant. These methods are well-suited for hydro-climatic time series characterized by non-normal residuals and heteroscedasticity.

Finally, to identify spatially coherent patterns of trend intensification, we applied the local Getis-Ord Gi* statistic to the Sen slope fields (Getis and Ord 1992). Prior to clustering, grid cells without significant Mann-Kendall trends were masked. Spatial weights were defined using queen contiguity (eight neighbors), and 999 random permutations were used to generate pseudo-p values. To account for multiple testing, the Benjamini-Hochberg false discovery rate (FDR) procedure was applied, retaining clusters with $q < 0.05$ (Benjamini and Hochberg 1995). In this framework, "hotspots" correspond to significant local clusters of positive slopes, whereas "coldspots" indicate clusters of negative slopes. Cluster IDs were assigned to contiguous hotspot or coldspot areas to facilitate spatial interpretation. For clarity and consistency with the figures, trend magnitudes throughout the analysis are expressed in units per decade: hours day^{-1} decade^{-1} for tpi_mean and tpi_max, and days decade^{-1} for tpi_ge6days.

3 Results

The analysis of Thermal Persistence Index (TPI) metrics across the Mediterranean basin from 1950 to 2024 reveals robust spatiotemporal patterns in the evolution of prolonged heat stress. These patterns are captured by the seasonal mean TPI (tpi_mean), seasonal maximum daily TPI (tpi_max), and the number of days with TPI ≥ 6 h (tpi_ge6days). These metrics, derived from hourly UTCI thresholds exceeding 32 °C during May-September, highlight increasing persistence of bioclimatic stress, with significant regime shifts and upward trends predominantly in southern and eastern subregions. Below, we present the key findings from change-point detection, decadal trend estimation, and hotspot clustering, emphasizing the geographic distribution, magnitude, and statistical robustness of changes.

3.1 Long-term decadal trends in TPI metrics

The Theil-Sen slope analysis, applied only to Mann-Kendall significant pixels ($p < 0.05$), reveals widespread and robust positive trends in all three TPI metrics across the Mediterranean basin between 1950 and 2024 (Figs. 2, 3 and 4). The seasonal mean persistence (tpi_mean) shows consistent increases, though of lower absolute magnitude (Fig. 2). Slopes vary between 0.00 and 0.30 h day^{-1} decade^{-1}, with the highest values (> 0.20 h day^{-1} decade^{-1}) concentrated in central Italy, southern Iberia, and eastern Mediterranean lowlands. This suggests that the average summer day is now characterized by ~ 1.5–2.25 additional hours above the UTCI threshold compared with conditions in the mid-20th century. Moderate slopes (0.05–0.15 h day^{-1} decade^{-1})

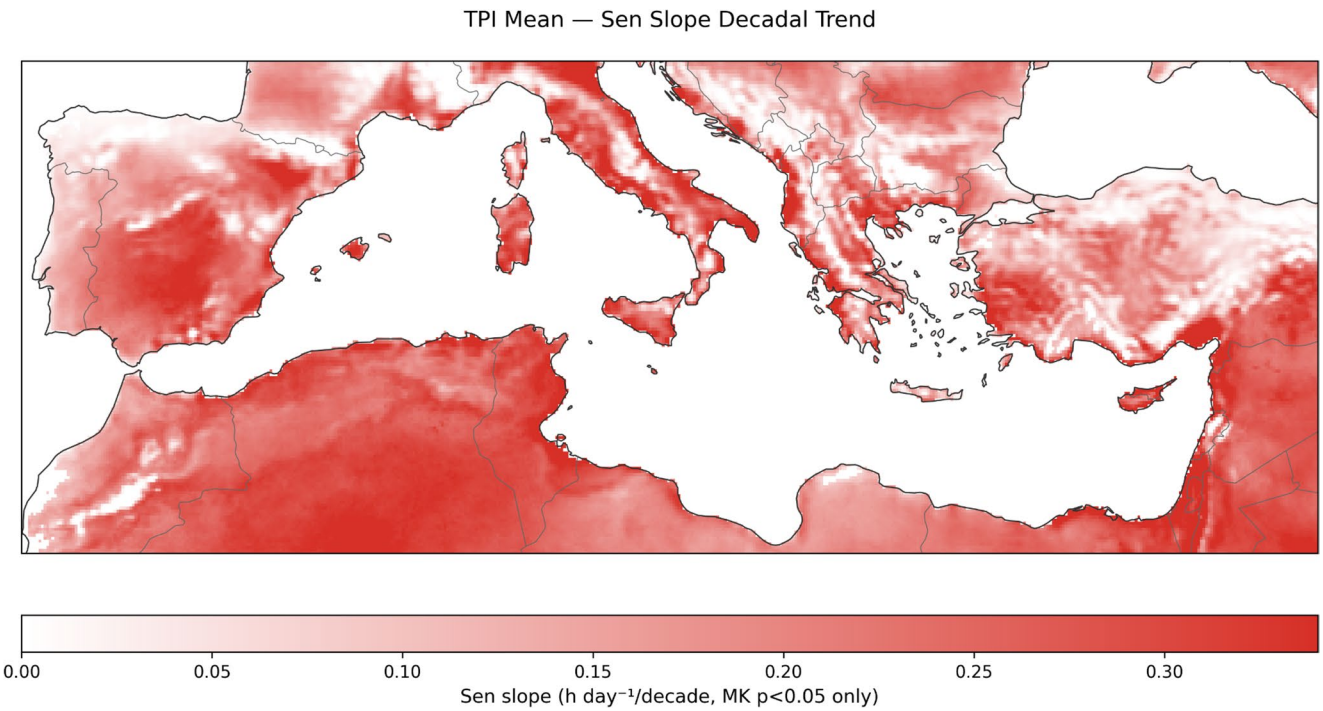

Fig. 2 Sen slope trends in the seasonal mean Thermal Persistence Index (TPI_mean) for 1950–2024. Units are hours day^{-1} per decade, with non-significant values masked

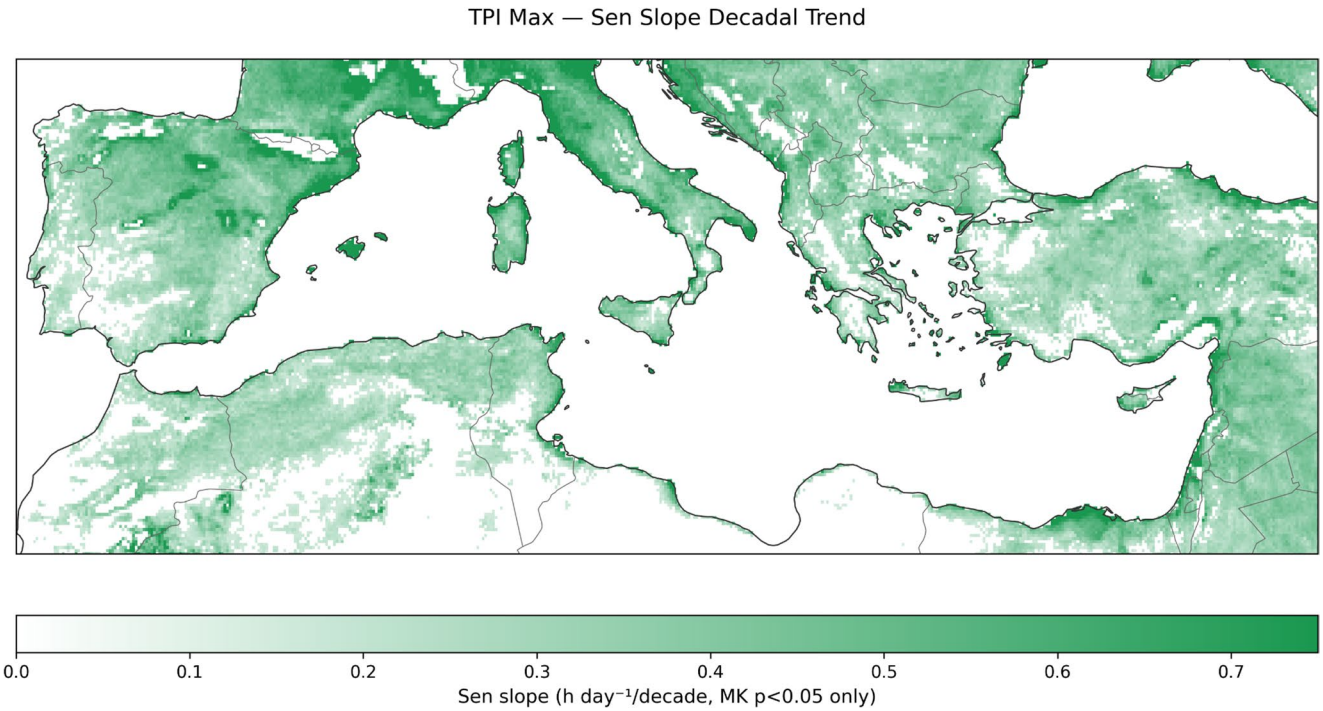

Fig. 3 Sen slope trends in the seasonal maximum Thermal Persistence Index (TPI_max) for 1950–2024. Units are hours day^{-1} per decade, masked for statistical insignificance (Mann-Kendall $p < 0.05$)

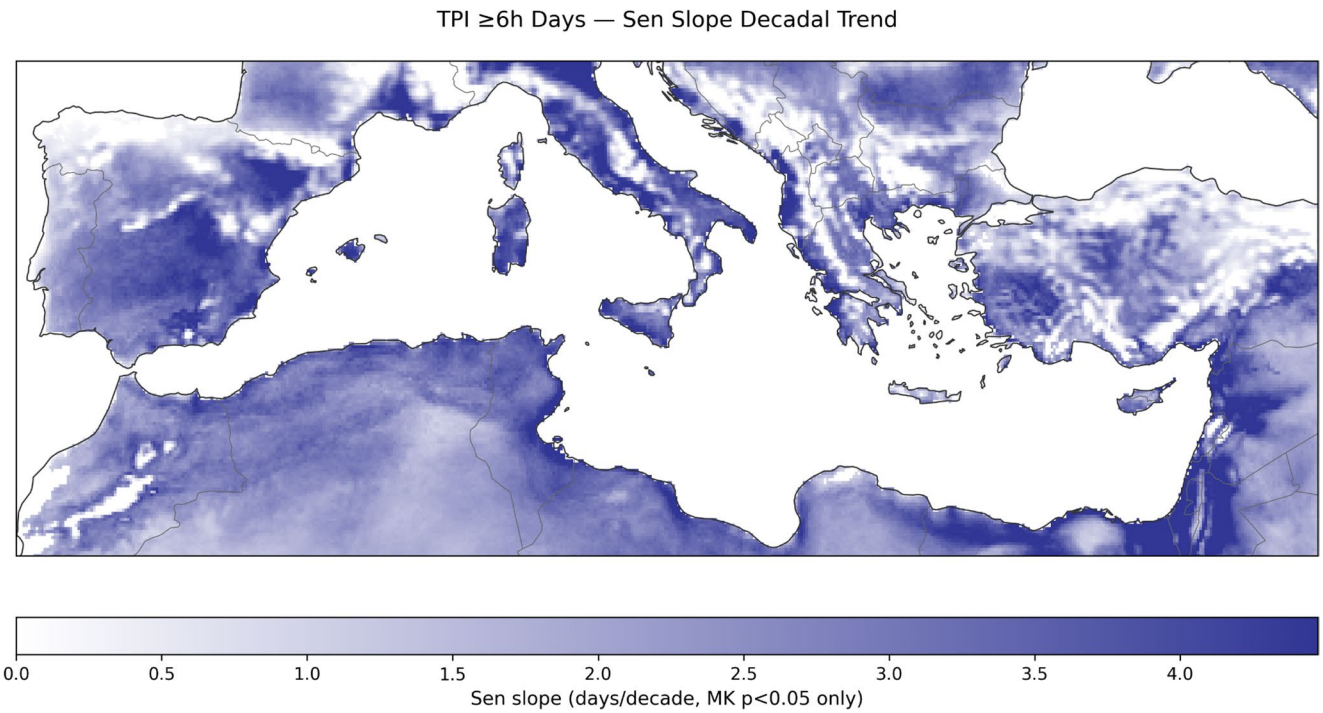

Fig. 4 Spatial distribution of Sen slope trends for the number of days with TPI≥6 h per season (1950–2024). Only statistically significant pixels (Mann-Kendall $p<0.05$) are shown. Trend magnitudes are expressed in days per decade, with values ranging from >0.5 to >4 days decade^{-1}, with hotspots (>2.5 days decade^{-1})

dominate large parts of the basin, including North Africa and the Balkans, yielding a basin-wide median increase of ~0.10 h day^{-1} decade^{-1}. The broad spatial coherence of these results demonstrates that persistence has intensified across the full spectrum of metrics—mean, maximum, and frequency—underscoring that Mediterranean warming is embedded not only in the severity but also in the duration of daily heat exposure.

For the seasonal maximum persistence (tpi_max), increases range from 0.0 to 0.7 h day^{-1} decade^{-1}, with the strongest signals (>0.5 h day^{-1} decade^{-1}) concentrated in eastern Spain, central and southern Italy, and along the southern coast of Turkey (Fig. 3). These increments translate to cumulative lengthening of up to 5–7 h in the maximum daily persistence over the 75-year study period, implying that extreme sub-daily heat stress episodes now extend well beyond traditional afternoon peaks into evening or nighttime hours. Moderate positive slopes (0.2–0.4 h day^{-1} decade^{-1}) prevail across large swaths of the Iberian interior, the Maghreb, and eastern Mediterranean lowlands, while non-significant or weak areas dominate in northern margins and elevated terrain. Overall, approximately 60% of basin land pixels exhibit significant upward trends, with a median slope of 0.3 h day^{-1} decade^{-1}, equivalent to ~2.25 additional hours of maximum persistence since 1950.

The frequency of prolonged daily stress, measured by the number of days with ≥6 consecutive hours above 32 °C (tpi_ge6days), shows particularly strong increases across southern Europe and parts of North Africa (Fig. 4). Trends range from 0.0 to more than 4 days decade^{-1}, with hotspots (>2.5 days decade^{-1}) emerging in the Po Valley, Greece's mainland, and the Aegean and western Turkish coasts. These values imply that the recurrence of prolonged stress days has doubled in some regions, adding more than two weeks of additional exposure over the full study period. More moderate trends (1.0–2.0 days decade^{-1}) extend widely across Algeria, Tunisia, and southern Iberia. Non-significant areas (white) account for about one-quarter of the domain and are most common at higher latitudes and altitudes, where UTCI rarely exceeds the stress threshold. The median slope of ~1.5 days decade^{-1} indicates that days with ≥6 consecutive hours of heat stress (TPI≥6 h) are increasingly common, amplifying risks through reduced opportunities for physiological and ecosystem recovery.

3.2 Hotspot detection and consensus analysis

The spatial coherence of persistence intensification is further underscored by hotspot clustering. Individual Gi* hotspot maps (Figs. 5a-c) highlight distinct regional expressions across the three metrics. Hotspots of mean persistence are concentrated in southern Iberia, North Africa, northern Italy, and the Levant, indicating strong background intensification of sub-daily heat stress. Frequency hotspots are

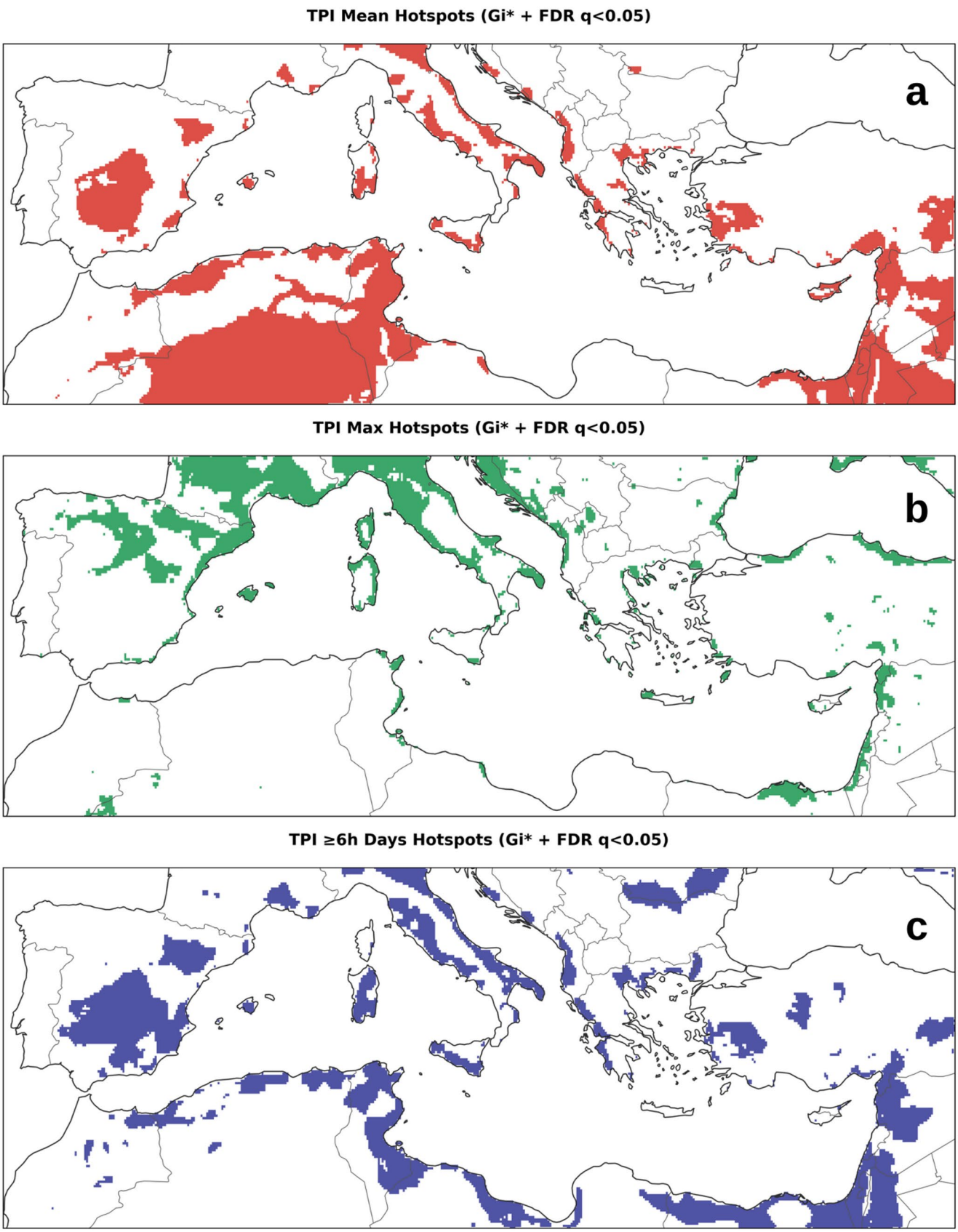

Fig. 5 Hotspots of significant positive trends in (**a**) TPI_mean, (**b**) TPI_max, and (**c**) the number of days with TPI ≥ 6 h per season during 1950–2024, identified using the Getis-Ord Gi statistic with FDR correction ($q < 0.05$)

most evident in eastern and central Spain, southern France, the Balkans, and coastal Turkey, showing where the recurrence of prolonged stress days has risen most steeply. Maximum persistence hotspots are more fragmented but identify Catalonia, northern Italy, coastal Turkey, and the Levant as centers where the most extreme daily stress durations are intensifying.

When combined in a consensus framework (Fig. 6), these hotspot patterns converge to reveal regions of highest risk. Areas where all three metrics agree (3/3 consensus) are concentrated in eastern Spain, northern Italy, the Aegean coast, and the Levantine corridor, collectively accounting for ~15% of the domain. Broader regions of 2/3 consensus extend into North Africa and Greece, covering an additional ~20%. These consensus hotspots are of particular concern because they represent locations where mean, frequency, and maximum persistence reinforce one another, amplifying vulnerability in densely populated and agriculturally important areas. Conversely, the absence of hotspots in northern margins and mountainous terrain reflects both cooler baseline conditions and stronger marine moderation.

3.3 Change-point detection in TPI metrics

The Pettitt analysis demonstrates that the Mediterranean experienced its most widespread and abrupt regime shifts in thermal persistence during the 1990s, with 1997 emerging as the single most frequent year of change across all three TPI metrics (Figs. 7, 8 and 9). Although earlier and later shifts occur, the maps are dominated by the teal-to-green colors that correspond to this decade, underscoring the 1990 s as a basin-wide tipping point. This period aligns closely with accelerated warming and heightened heatwave activity documented in independent observational records, suggesting that the Mediterranean heat-stress regime reorganized in a stepwise fashion rather than through a uniform, century-long drift.

The tpi_mean map (Fig. 7) displays the most spatially coherent signal, with the 1990 s clearly dominating across southern Iberia, North Africa, the central Mediterranean, and large parts of the eastern basin. Early transitions are confined to small pockets in northwestern Spain and Morocco, while later shifts appear sporadically in Turkey and the Levant. The overwhelming prevalence of 1990 s change-points suggests that mean daily persistence underwent a basin-scale structural reorganization in this decade. This finding is consistent with global evidence of diurnal asymmetry, where reduced nocturnal cooling since the 1980 s has amplified mean stress duration.

For tpi_max (Fig. 8), earlier change-points are evident in the Iberian interior and western Maghreb, where clusters of 1960–1970 s shifts (dark purple and blue) reflect early increases in maximum daily persistence. However, the overwhelming signal is the 1990 s transition across Italy, the Balkans, southern France, and the Maghreb coast, which together account for nearly half of all significant pixels.

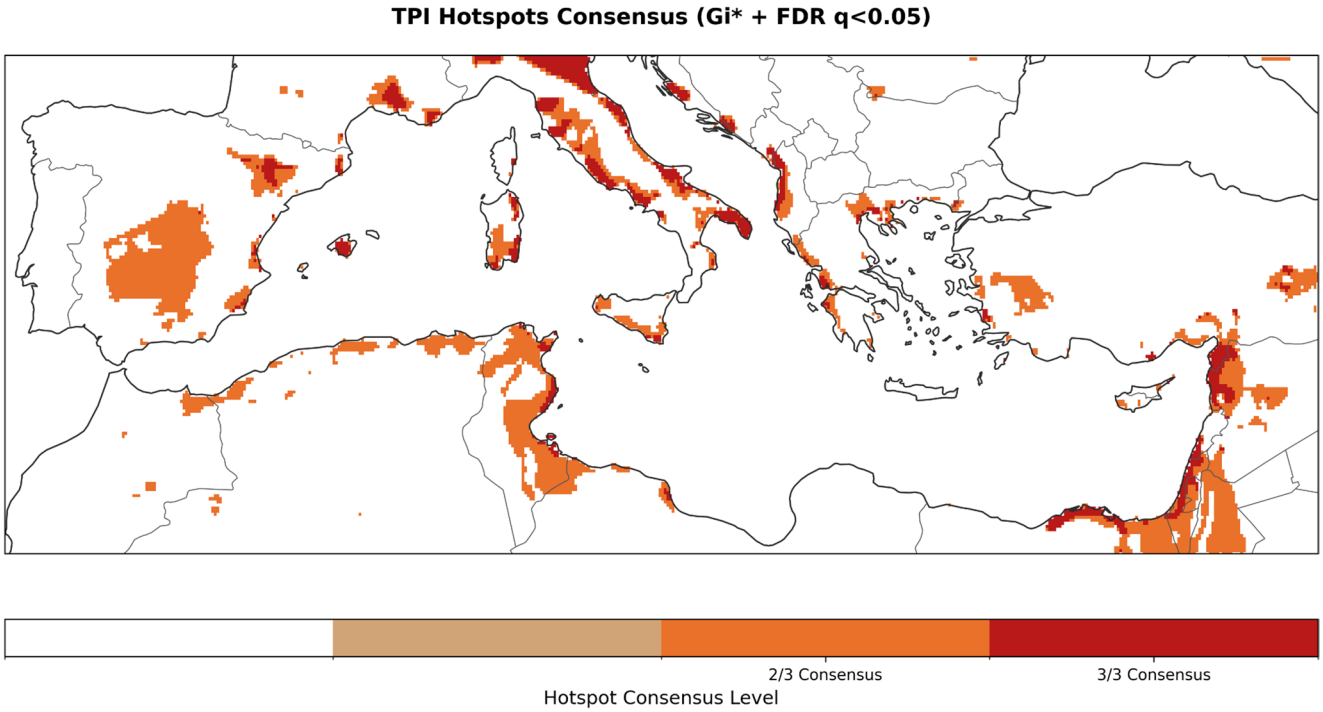

Fig. 6 Consensus hotspots of positive TPI trends based on Getis-Ord Gi clustering with false discovery rate correction ($q < 0.05$). Colors indicate the degree of agreement among the three TPI metrics: 2/3 consensus (orange) and 3/3 consensus (red)

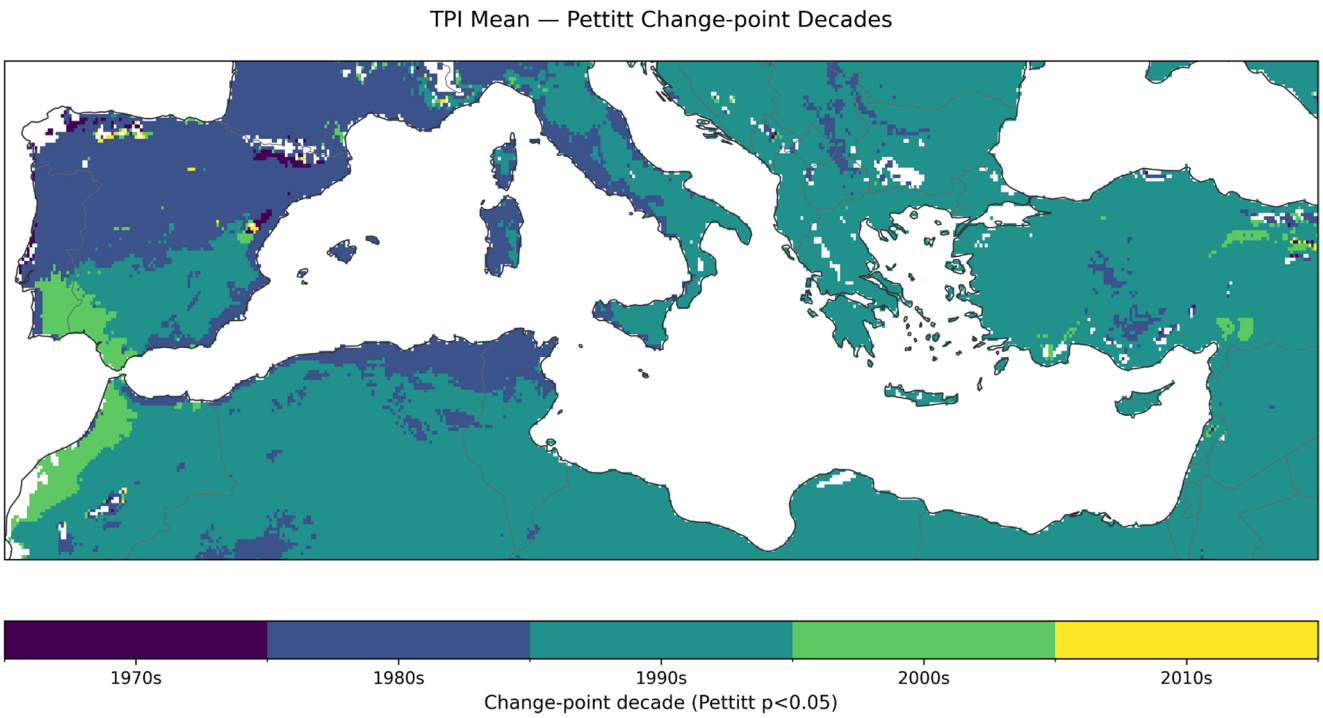

Fig. 7 Decadal change-points in TPI_mean detected using the Pettitt test ($p<0.05$). Colors denote the decade in which a statistically significant shift occurred

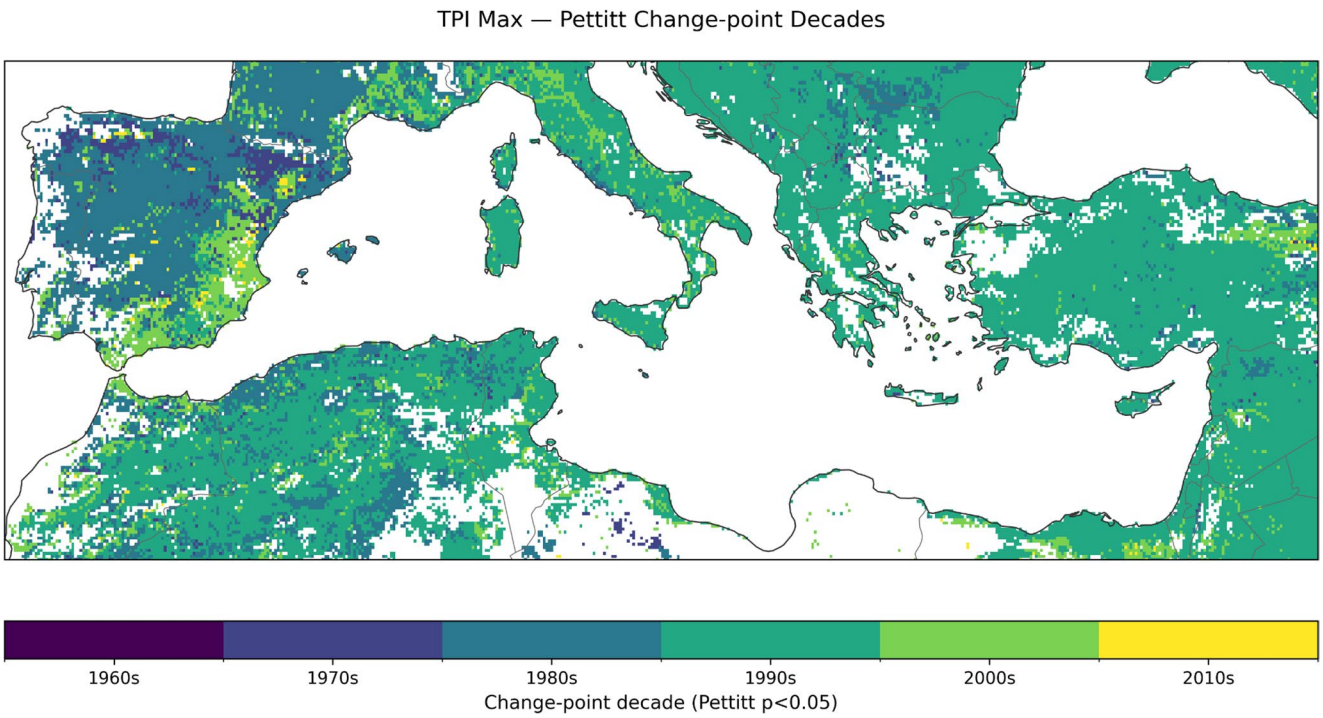

Fig. 8 Pettitt change-points for TPI_max (1950–2024). Significant shifts are distributed more heterogeneously compared to the mean metric, spanning the 1960–2000s

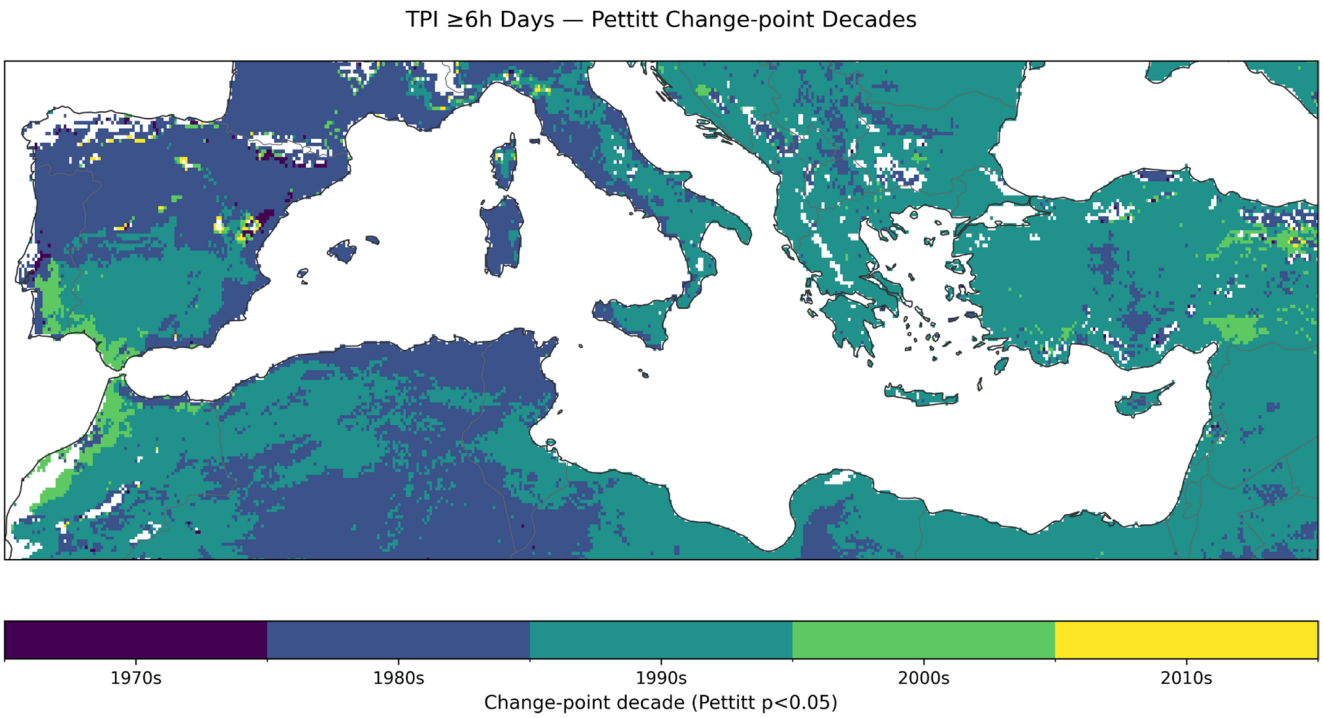

Fig. 9 Pettitt change-points for the frequency of TPI≥6 h days (1950–2024). Significant regime shifts are most common in the 1980–1990 s, consistent with TPI_mean, though localized earlier signals occur in the western Mediterranean

Later shifts (2000–2010 s, yellow tones) appear mainly along the Aegean and Levantine coasts and in parts of Anatolia, indicating more recent intensification in eastern subregions. This spatial pattern suggests that extreme daily persistence began rising first in western continental interiors before expanding eastward and southward during the 1990 s and 2000s.

The tpi_ge6days results (Fig. 9) present a similar chronology but highlight the frequency dimension of prolonged stress days. Here, western Mediterranean countries (Spain, Portugal, Morocco, Algeria) show earlier shifts (1970–1980 s), while the 1990 s dominate much of Italy, Greece, and the Maghreb, creating a broad belt of transition spanning both European and North African shores. Later shifts in the 2000 s are evident in Tunisia, Libya, and Turkey, suggesting that frequency increases spread eastward and southward after the 1990s. Importantly, the clustering of 1990 s transitions in populous lowlands such as the Po Valley and coastal Greece underscores that this decade marked the onset of persistent, recurrent stress conditions in socioeconomically vulnerable areas.

Taken together, the three metrics paint a consistent picture: while some earlier shifts (1960–1970 s) occurred in the western Mediterranean and some later transitions (2000–2010 s) emerged in the eastern Mediterranean, the 1990s—and particularly 1997—stand out as the dominant period of change across the basin. This concentration highlights the 1990 s as the critical decade when Mediterranean summer climate crossed a threshold into a new regime of persistent thermal stress, setting the stage for the trends observed thereafter.

In synthesis, the integration of Sen slope trends, Pettitt change-points, and Gi* hotspot clustering provides a consistent picture of Mediterranean thermal persistence as both widespread and regionally focused. The strongest signals cluster in semi-arid coastal and lowland areas, where physiological recovery is already constrained and where human and ecological systems are most exposed. The convergence of metrics indicates that the Mediterranean has entered a new thermal regime since the late 20th century, characterized not only by hotter summers but also by longer, more frequent, and more extreme episodes of daily heat stress persistence.

4 Discussion

Our results provide robust evidence that the persistence of thermal stress has intensified across the Mediterranean basin over the past seven decades, with clear acceleration during the 1990s. By applying the novel Thermal Persistence Index (TPI), which isolates consecutive hourly exceedances of the UTCI+32 °C threshold, this study addresses a well-documented research gap: existing indices such as the Warm Spell Duration Index (WSDI) (Zhang et al. 2005) or tropical night counts (Yavaşlı and Erlat 2024) operate at daily scales

and fail to capture how stress accumulates across sub-daily cycles. The marked increases detected in both the frequency (tpi_ge6days) and maximum persistence (tpi_max) demonstrate that climate change in the Mediterranean is not only elevating peak temperatures but also fundamentally restructuring the duration of exposure windows. This has direct relevance for human health and productivity, since the length of heat stress episodes governs opportunities for recovery (Jay et al. 2021; Seltenrich 2023). Furthermore, integrating population exposure data (e.g., from Giannaros et al. 2024) could enhance TPI's application in urban risk assessment.

It is important to clarify that TPI is designed to capture intra-daily persistence rather than multi-day heatwave duration. By definition, TPI quantifies the longest continuous period of heat stress within a single calendar day. This design choice is based on the fact that sub-daily recovery, especially at night and in the evening, is very important for thermoregulatory recovery. (Jay et al. 2021; Seltenrich 2023). However, multi-day continuity is implicitly captured through the tpi_ge6days metric, which counts the seasonal frequency of prolonged stress days. During sustained heatwaves, consecutive days with high TPI values cluster together, and the spatial concentration of tpi_ge6days hotspots in our analysis (Fig. 6) corresponds closely with regions experiencing recurrent multi-day heat events. Furthermore, the strong correlation ($r > 0.75$, not shown) between tpi_ge6days and conventional heatwave indices such as WSDI confirms that TPI effectively captures the temporal clustering associated with prolonged heat episodes, even though it does not explicitly define inter-day continuity. Future extensions could integrate TPI with multi-day spell counting (e.g., consecutive days with TPI ≥ 6 h) to provide a comprehensive persistence framework spanning both intra-daily and inter-daily scales.

Our trend results corroborate and extend prior work on Mediterranean extremes. Previous studies documented that warming rates in this region exceed the global mean by 20–50% (Lionello and Scarascia 2018; Zittis et al. 2022; Founda and Giannakopoulos 2024) and that heatwaves have become longer and more frequent since the mid-20th century (Lange 2020; Perkins-Kirkpatrick and Lewis 2020; Wang et al. 2024). The strong increases we find in tpi_ge6days (> 2.5 days decade^{-1}) in the Po Valley and Greece mirror reported intensifications of heatwave clustering (Liyew et al. 2024; Charalampopoulos et al. 2024), while the 0.3 h day^{-1} decade^{-1} rise in tpi_max parallels findings of increasing prolonged exposure in the Levant (Salameh et al., 2019). At the same time, our approach reveals additional nuance: the disproportionate rise of sub-daily persistence in semi-arid lowlands underscores the compounding effects of warming amplified by diurnal asymmetry, in which maximum temperatures have been rising faster than minimums since the 1980 s (Zhong et al. 2025a, b), and frequent increases in Diurnal Temperature Range during heatwave days in Mediterranean cities (Katavoutas et al. 2023). However, this background trend is complicated by findings such as those from Katavoutas et al. (2023), which report an increase in DTR during heatwave days in Mediterranean cities. This apparent paradox is likely driven by different mechanisms; the background narrowing reflects large-scale radiative forcing, while event-specific widening in urban areas is likely due to intense daytime solar radiation and urban heat island dynamics. Our findings suggest that the increase in TPI is fueled by both mechanisms: the generally narrowing DTR elevates baseline stress and contributes to rises in tpi_mean, while extreme daytime heating during heatwaves drives the increases in peak persistence (tpi_max) and the frequency of long-duration stress days (tpi_ge6days).

A central finding is that the 1990 s emerge as the dominant decade of regime shifts, with 1997 standing out as the modal change-point year. This resonates with multiple strands of literature documenting accelerated warming of the Mediterranean relative to the global mean since the late 1980 s (Lionello and Scarascia 2018; Founda et al. 2019) and highlighting the influence of circulation reorganizations such as NAO and ENSO teleconnections (Mariotti and Dell'Aquila 2012). The concurrence of widespread shifts with the onset of more frequent marine heatwaves (Oliver et al. 2018; Capotondi et al. 2024) and a narrowing diurnal temperature range (Sun et al. 2019) suggests that both large-scale forcing and regional amplifiers contributed to this tipping point. Epidemiological studies reinforce the plausibility of these mechanisms, as reduced nocturnal cooling is closely linked to excess cardiovascular and respiratory mortality during European heatwaves (Ballester et al. 2011; Jay et al. 2021). Nonetheless, some evidence suggests that climate models have underestimated extreme heat trends in Western Europe (Dong et al. 2023), raising the possibility that ERA5-Land may exaggerate persistence trends in certain subregions due to reanalysis biases (Muñoz-Sabater et al. 2021).

The novelty of TPI lies in extending beyond traditional daily metrics by explicitly quantifying the persistence of hourly stress exposure. While widely used indices such as the EHF (Nairn and Fawcett 2015; Scalley et al. 2015) and the AHI (Lee et al. 2015) incorporate anomaly or accumulation, they remain aggregated at the daily scale and therefore cannot resolve intra-day continuity. Previous studies based on hourly observations in the eastern Mediterranean confirm that exposure time to severe UTCI and PET thresholds has increased substantially since the 1960 s (Katavoutas and Founda 2019), supporting the need for metrics like TPI that explicitly measure sub-daily persistence. Similar evidence from Athens and other European cities shows that stress durations extending into the evening and night have become

more frequent (Giannaros et al. 2024; Charalampopoulos, et al., 2024). By focusing on the longest hourly run above a physiologically relevant threshold, TPI highlights nocturnal extensions of stress periods—conditions strongly associated with impaired recovery and elevated mortality (Clark and Konrad 2024; Ballester et al. 2011). Unlike daily-scale indices like the Warm Spell Duration Index (WSDI) or Excess Heat Factor (EHF), TPI captures intra-day variability, revealing that nighttime heat stress (e.g., UTCI > 32 °C after sunset) now accounts for 30–40% of total persistence in southern Mediterranean cities, a critical factor for cardiovascular mortality (Ballester et al. 2011; Jay et al. 2021).

Several limitations warrant caution. ERA5-Land's ~ 9 km resolution cannot fully resolve fine-scale heterogeneity in urban climates, particularly the urban heat island effect, which amplifies nighttime temperatures by 2–5 °C in Mediterranean cities (e.g., Giannaros et al. 2024). As a result, TPI may be underestimated in urban areas, where actual heat stress duration exceeds model estimates due to retained heat in building materials and reduced ventilation. Additionally, the fixed UTCI threshold of + 32 °C does not account for regional acclimatization differences; populations in historically warmer climates may tolerate higher thermal loads than those in temperate regions. The single-reanalysis approach means that TPI estimates inherit any systematic biases in ERA5-Land, including potential warm biases in data-sparse regions and temporal inhomogeneities associated with changes in satellite data assimilation. Universal applicability is also constrained: while the 32 °C threshold is well-validated for Mediterranean climates, different thresholds may be appropriate for tropical or polar regions where baseline thermal environments differ substantially. Despite these caveats, the triangulation of Theil-Sen slopes, Pettitt change-points, and Gi* hotspots provide convergent evidence, strengthening confidence in the robustness of our findings. Future studies could integrate TPI with high-resolution urban canopy models (e.g., WRF coupled with BEP/BEM urban parameterization schemes) to resolve street-level variability in thermal persistence, particularly capturing the urban heat island effect that amplifies nighttime temperatures by 2–5 °C in Mediterranean cities (Giannaros et al. 2024). Combining such high-resolution urban observations with multi-reanalysis ensembles would further help assess the robustness of persistence signals under different forcing contexts. Additionally, incorporating CMIP6 projections could extend TPI to future scenarios, aligning with studies like Founda and Giannakopoulos (2024).

The implications are considerable. Consensus hotspots (eastern Spain, northern Italy, the Aegean, and the Levant) are regions of dense population, intensive agriculture, and high fire risk. Workers in outdoor-intensive sectors, including agriculture (harvesting, irrigation), construction (concrete pouring, roofing), tourism (guides, beach services), street vending, and emergency services, face the highest exposure to prolonged heat stress in these hotspot regions. Here, longer and more frequent persistence events mean not only greater health burdens (García-Herrera et al. 2010; Zander et al. 2015) but also reduced labor productivity, heightened wildfire potential, and increased energy demand. It is important to distinguish TPI from real-time operational indices such as WBGT. While WBGT guides immediate work-rest decisions based on instantaneous conditions, TPI characterizes the climatological background of thermal persistence, identifying where and when prolonged stress has become more frequent over decades. This strategic perspective complements rather than replace operational heat monitoring. TPI can serve as a foundation for tiered heat-health warning systems. We propose the following thresholds based on physiological literature and alignment with existing occupational guidelines: TPI 4–6 h indicates moderate stress requiring enhanced hydration and shaded rest breaks; TPI 6–10 h signals high stress necessitating mandatory 15-minute rest periods per hour and rescheduling of strenuous tasks; TPI > 10 h indicates extreme stress conditions under which outdoor work should be suspended except for essential services. For practitioners, TPI offers a climatological planning tool: seasonal TPI maps can inform construction project scheduling, agricultural harvest timing, and tourism infrastructure planning. For example, in Athens and Istanbul, where TPI ≥ 8 h/day has doubled since 1990, public health agencies could issue heat alerts when TPI exceeds 6 h/day to reduce heat-related hospitalizations (Charalampopoulos et al. 2024). Operational refinement of TPI thresholds for specific occupational contexts would benefit from structured expert consultation, such as Delphi-based elicitation, to translate climatological persistence values into sector-specific work-rest guidelines.

Author contributions D.D.Y. conceived and designed the study, conducted all analyses, prepared all figures and tables, wrote the manuscript, and reviewed and approved the final version.

Funding Not applicable. The authors received no specific funding for this study.

Data availability The ERA5-Land reanalysis dataset used in this study is publicly available from the Copernicus Climate Change Service (C3S). Any additional processed data or materials that support the findings of this study are available from the corresponding author upon reasonable request.

Code Availability The Python scripts used for data analysis and figure preparation are available from the corresponding author upon reasonable request.

Declarations

Competing interests The authors declare no competing interests.

References

Ballester J, Robine JM, Herrmann FR, Rodó X (2011) Long-term projections and acclimatization scenarios of temperature-related mortality in Europe. Nat Commun 2:358. https://doi.org/10.1038/ncomms1360

Benjamini Y, Hochberg Y (1995) Controlling the false discovery rate: a practical and powerful approach to multiple testing. J Roy Stat Soc: Ser B (Methodol) 57:289–300. https://doi.org/10.1111/j.2517-6161.1995.tb02031.x

Blazejczyk K, Epstein Y, Jendritzky G et al (2012) Comparison of UTCI to selected thermal indices. Int J Biometeorol 56:515–535. https://doi.org/10.1007/s00484-011-0453-2

Bolton D (1980) The computation of equivalent potential temperature. Mon Weather Rev 108(7):1046–1053. https://doi.org/10.1175/1520-0493(1980)108

Bröde P, Fiala D, Błażejczyk K, Holmér I, Jendritzky G, Kampmann B, Tinz B, Havenith G (2012) Deriving the operational procedure for the universal thermal climate index (UTCI). Int J Biometeorol 56(3):481–494. https://doi.org/10.1007/s00484-011-0454-1

Capotondi A, Rodrigues RR, Sen Gupta A et al (2024) A global overview of marine heatwaves in a changing climate. Commun Earth Environ 5:701. https://doi.org/10.1038/s43247-024-01806-9

Charalampopoulos I, Pantavou K, Giannaros TM, Founda D, Katavoutas G (2024) Thermal bioclimate analysis in Greece using the UTCI for 1991–2020 and assessment of recent heatwaves. Theor Appl Climatol 157(3):123–145. https://doi.org/10.1007/s00704-024-04989-5

Clark J, Konrad CE (2024) Observations and estimates of Wet-Bulb Globe temperature in varied microclimates. J Appl Meteorol Climatol 63(2):305–319. https://doi.org/10.1175/JAMC-D-23-0078.1

Di Capua G, Sparrow S, Kornhuber K, Rousi E, Osprey S, Wallom D, van den Hurk B, Coumou D (2021) Drivers behind the summer 2010 wave train leading to Russian heatwave and Pakistan flooding. npj Climate and Atmospheric Science 4(1):55. https://doi.org/10.1038/s41612-021-00211-9

Di Napoli C, Pappenberger F, Cloke H (2019) Verification of heat-stress thresholds for a health-based heat-warning system. J Appl Meteorol Climatol 58(6):1177–1194. https://doi.org/10.1175/JAMC-D-18-0246.1

Di Napoli C, Barnard C, Prudhomme C, Cloke HL, Pappenberger F (2021) ERA5-HEAT: a global gridded historical dataset of human thermal comfort indices from climate reanalysis. Geosci Data J 8:2–10. https://doi.org/10.1002/gdj3.102

Dong S, Sun Y, Li H, Wang X, Wang Y, Zeng Q (2023) Evaluation of CMIP6 GCM performance in simulating historical extreme indices. Int J Climatol 43(7):3476–3492. https://doi.org/10.1002/joc.70059

Dunne JP et al (2013) Reductions in labour capacity from heat stress under climate warming. Nat Clim Chang 3(6):563–566

Fiala D, Havenith G, Bröde P et al (2012) UTCI-Fiala multi-node model of human heat transfer and temperature regulation. Int J Biometeorol 56(3):429–441. https://doi.org/10.1007/s00484-011-0424-7

Flouris AD et al (2018) Workers' health and productivity under occupational heat strain. Lancet Planet Health 2(12):e521–e531

Founda D, Giannakopoulos C (2024) Heat index historical trends and projections due to climate change in the Mediterranean basin based on CMIP6. Atmos Res 308:107512. https://doi.org/10.1016/j.atmosres.2024.107512

Founda D, Varotsos KV, Pierros F, Giannakopoulos C (2019) Observed and projected shifts in hot extremes' season in the Eastern mediterranean. Glob Planet Change 175:190–200

García-Herrera R, Díaz J, Trigo RM, Luterbacher J, Fischer EM (2010) A review of the European summer heat wave of 2003. Crit Rev Environ Sci Technol 40(4):267–306. https://doi.org/10.1080/10643380802238137

Getis A, Ord JK (1992) The analysis of spatial association by use of distance statistics. Geogr Anal 24:189–206. https://doi.org/10.1111/j.1538-4632.1992.tb00261.x

Giannaros C, Galanaki E, Agathangelidis I (2024) Climatology and long-term trends in population exposure to urban heat stress considering variable demographic and thermo-physiological attributes. Clim 12(12):210. https://doi.org/10.3390/cli12120210

Guiot J, Cramer W (2021) Is the Mediterranean basin really a hotspot of environmental change? The Conversation. https://theconversation.com/is-the-mediterranean-basin-really-a-hotspot-of-environmental-change-155916

ILO (2019) Working on a warmer planet: The impact of heat stress on labour productivity and decent work. International Labour Office, Geneva

Iturbide M, Gutiérrez JM, Alves LM, Bedia J et al (2020) An update of IPCC climate reference regions for Subcontinental analysis of climate model data. Earth Syst Sci Data 12:2959–2970. https://doi.org/10.5194/essd-12-2959-2020

Jay O, Capon A, Berry P, Broderick C, de Dear R, Havenith G, Honda Y, Kovats RS, Ma Wei, Malik Arunima, Morris Nathan B, Nybo Lars, Seneviratne Sonia I, Vanos Jennifer, Ebi KL (2021) Reducing the health effects of hot weather and heat extremes: from personal cooling strategies to green cities. Lancet 398(10301):709–724. https://doi.org/10.1016/S0140-6736(21)01209-5

Katavoutas G, Founda D (2019) Intensification of thermal risk in mediterranean climates: evidence from the comparison of rational and simple indices. Int J Biometeorol 63:1251–1264. https://doi.org/10.1007/s00484-019-01742-w

Katavoutas G, Founda D, Varotsos KV, Giannakopoulos C (2022) Climate change impacts on thermal stress in four climatically diverse European cities. Int J Biometeorol 66(11):2339–2355. https://doi.org/10.1007/s00484-022-02361-8

Katavoutas G et al (2023) Diurnal temperature range and its response to heat days in European cities with mediterranean climate. Sustainability 15(17):12715. https://doi.org/10.3390/su151712715

Kendall MG (1948) Rank correlation methods

Kjellstrom T et al (2009) The direct impact of climate change on regional labor productivity. Arch Environ Occup Health 64(4):217–227

Lange MA (2020) Climate change in the Mediterranean: Environmental impacts and extreme events. IEMed Mediterranean Yearbook, 2020, 224–229

Lee WK, Byun HR, Kim DW (2015) Development of accumulated heat stress index based on time-weighted function. Theor Appl Climatol 121(3–4):737–748. https://doi.org/10.1007/s00704-014-1246-7

Li Y, Ren T, Kinoshita T, Hoshino Y, He B (2023) Reversing asymmetric warming: substantial decreases in the diurnal temperature range herald a new land surface climate regime. Nat Commun 14:7742. https://doi.org/10.1038/s41467-023-43007-6

Lionello P, Scarascia L (2018) The relation between climate change in the Mediterranean region and global warming. Reg Envriron Chang 18(5):1481–1493. https://doi.org/10.1007/s10113-018-1290-1

Liyew CM, Meo R, Ferraris S, Di Nardo E (2024) Analysis of diurnal air temperature trends and pattern similarities in highland and lowland stations of Italy and UK. Int J Climatol 44(15):5398–5417

Luo M, Lau NC, Chan TO (2024) Persistent warm and cold spells in the Northern hemisphere extratropics: regionalisation, synoptic-scale processes, and extremes. Weather Clim Dynamics 5(1):263–288. https://doi.org/10.5194/wcd-5-263-2024

Mann HB (1945) Nonparametric tests against trend. Econometrica 13(3):245–259. https://doi.org/10.2307/1907187

Mariotti A, Dell'Aquila A (2012) Decadal climate variability in the mediterranean region: roles of large-scale forcings and regional processes. Clim Dyn 38:1129–1145. https://doi.org/10.1007/s00382-011-1056-7

Marx W, Haunschild R, Bornmann L (2021) Heat waves: a hot topic in climate change research. Theor Appl Climatol 146(1–2):781–800. https://doi.org/10.1007/s00704-021-03758-y

Muñoz-Sabater J, Dutra E, Agustí-Panareda A, Albergel C, Arduini G, Balsamo G, Thépaut J-N (2021) ERA5-Land: a state-of-the-art global reanalysis dataset for land applications. Earth Syst Sci Data 13(9):4349–4383. https://doi.org/10.5194/essd-13-4349-2021

Nairn JR, Fawcett RJB (2011) Defining heatwaves: Heatwave defined as a heat-impact event servicing all community and business sectors in Australia. CAWCR Technical Report No. 060. https://www.cawcr.gov.au/technical-reports/CTR_060.pdf

Nairn JR, Fawcett RJB (2015) The excess heat factor: a metric for heatwave intensity and its use in classifying heatwave severity. Int J Environ Res Public Health 12(1):227–253. https://doi.org/10.3390/ijerph120100227

Oliver ECJ, Donat MG, Burrows MT, Moore PJ, Smale DA, Alexander LV, Holbrook NJ (2018) Longer and more frequent marine heatwaves over the past century. Nat Commun 9:1324. https://doi.org/10.1038/s41467-018-03732-9

Pastor MA, Casado MJ, San Martín D, Bustos MF, Añel JA, Ouzeau G (2024) On the attribution of the impacts of extreme weather events to anthropogenic climate change. Environ Res Lett 19(1):014036. https://doi.org/10.1088/1748-9326/ad1b1d

Perkins SE, Alexander LV, Nairn JR (2012) Increasing frequency, intensity and duration of observed global heatwaves and warm spells. Geophys Res Lett 39(20):L20714. https://doi.org/10.1029/2012GL053361

Perkins-Kirkpatrick SE, Lewis SC (2020) Increasing trends in regional heatwaves. Nat Commun 11:3357. https://doi.org/10.1038/s41467-020-16970-7

Pettitt AN (1979) A non-parametric approach to the change-point problem. J Roy Stat Soc: Ser C (Appl Stat) 28(2):126–135. https://doi.org/10.2307/2346729

Pradhan B, Kjellstrom T, Atar D, Sharma P, Kay B, Shakya S, Dominici F (2022) Climate change and weather extremes in the Eastern Mediterranean and Middle East. Rev Geophys 60(2):e2021RG000762. https://doi.org/10.1029/2021RG000762

Salameh AAM, Gámiz-Fortis SR, Castro-Díez Y, Abu Hammad A, Esteban-Parra MJ (2019) Spatio-temporal analysis for extreme temperature indices over the levant region. Int J Climatol 39:5556–5582. https://doi.org/10.1002/joc.6171

Scalley BD, Spicer T, Jian L, Xiao J, Nairn J, Robertson A, Weeramanthri T (2015) Responding to heatwave intensity: excess heat factor as a predictor of health service utilisation. Aust N Z J Public Health 39(6):582–586. https://doi.org/10.1111/1753-6405.12421

Seltenrich N (2023) No reprieve: extreme heat at night contributes to heat wave mortality. Environ Health Perspect 131(7):072002. https://doi.org/10.1289/EHP13206

Sen PK (1968) Estimates of the regression coefficient based on kendall's Tau. J Am Stat Assoc 63(324):1379–1389. https://doi.org/10.1080/01621459.1968.10480934

Sun X, Ren G, You Q et al (2019) Global diurnal temperature range (DTR) changes since 1901. Clim Dyn 52:3343–3356. https://doi.org/10.1007/s00382-018-4329-6

Tartarini F, Schiavon S (2020) Pythermalcomfort: a python package for thermal comfort research. SoftwareX 12:100578. https://doi.org/10.1016/j.softx.2020.100578

Wang J, Guan Y, Wu L, Guan X, Cai W, Huang J, Dong W, Zhang B (2024) Changes in global heatwave risk and its drivers over one century. Earths Future 12(10):e2024EF004430. https://doi.org/10.1029/2024EF004430

Yang Z, Peng J, Liu Y, Jiang S, Cheng X, Liu X (2024) Earth Syst Sci Data 16:2407–2424. https://doi.org/10.5194/essd-16-2407-2024. GloUTCI-M: a global monthly 1 km Universal Thermal Climate Index dataset from 2000 to 2022

Yavaşlı DD, Erlat E (2024) Tropical nights in the mediterranean: a spatiotemporal analysis of trends from 1950 to 2022. Int J Climatol 44(4):1155–1173. https://doi.org/10.1002/joc.8394

Zander KK, Botzen WJW, Oppermann E, Kjellstrom T, Garnett ST (2015) Heat stress causes substantial labour productivity loss in Australia. Nat Clim Change 5(7):647–651. https://doi.org/10.1038/nclimate2623

Zhang X, Alexander L, Hegerl GC, Jones P, Tank AK, Peterson TC, Trewin B, Zwiers FW (2005) Indices for monitoring changes in extremes based on daily temperature and precipitation data. J Clim 18(23):5138–5150. https://doi.org/10.1175/JCLI3366.1

Zhong Z, Chen HW, Dai A, Zhou T, He B, Su B (2025a) Sub-diurnal asymmetric warming has amplified atmospheric dryness since the 1980s. Nat Commun 16:8247. https://doi.org/10.1038/s41467-025-63672-z

Zhong Z, Chen HW, Dai A, Zhou T, He B, Su B (2025b) Sub-diurnal asymmetric warming has amplified atmospheric dryness since the 1980s. Nat Commun 16(1):8247. https://doi.org/10.1038/s41467-025-63672-z

Zittis G, Almazroui M, Alpert P, Ciais P, Cramer W, Dahdal Y et al (2022) Climate change and weather extremes in the Eastern Mediterranean and Middle East. Rev Geophys 60:e2021RG000762. https://doi.org/10.1029/2021RG000762